ACS chemical biology

Articles

pubs.acs.org/acschemicalbiology

Identification of PDE6D as a Molecular Target of Anecortave Acetate *via* a Methotrexate-Anchored Yeast Three-Hybrid Screen

Allan R. Shepard,*[,†] Raymond E. Conrow,[†] Iok-Hou Pang,[†] Nasreen Jacobson,[†] Mandana Rezwan,[‡] Katrin Rutschmann,[‡] Daniel Auerbach,[‡] Rohitha SriRamaratnam,[§] and Virginia W. Cornish*[,§]

[†]Alcon, a Novartis Company, Fort Worth, Texas 76134, United States

[‡]Dualsystems Biotech AG, Schlieren, Switzerland

[§]Department of Chemistry, Columbia University, New York, New York 10027, United States

Supporting Information

ABSTRACT: Glaucoma and age-related macular degeneration are ocular diseases targeted clinically by anecortave acetate (AA). AA and its deacetylated metabolite, anecortave desacetate (AdesA), are intraocular pressure (IOP)-lowering and angiostatic cortisenes devoid of glucocorticoid activity but with an unknown mechanism of action. We used a methotrexate-anchored yeast three-hybrid (Y3H) technology to search for binding targets for AA in human trabecular meshwork (TM) cells, the target cell type that controls IOP, a major risk factor in glaucoma. Y3H hits were filtered by competitive Y3H screens and coimmunoprecipitation experiments and verified by surface plasmon resonance analysis to yield a single target, phosphodiesterase 6-delta (PDE6D). PDE6D is a prenyl-binding protein with additional function outside the PDE6 phototransduction system. Overexpression of PDE6D in mouse eyes caused elevated IOP, and this elevation was reversed by topical ocular application of either AA or AdesA. The identification of PDE6D as the molecular binding partner of AA provides insight into the role of this drug candidate in treating glaucoma.

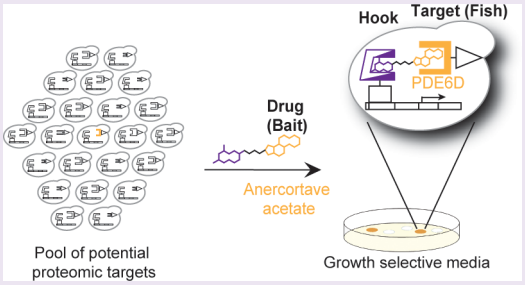

Anecortave acetate (AA) is a compound that has been the subject of considerable interest as an intraocular pressure (IOP)-lowering agent for treating glaucoma.[1−4] AA showed sustained IOP-lowering activity with no serious adverse events when delivered as a single injection under the surface membrane (bulbar conjunctiva) on the front of the eye.[2−4] AA was also explored earlier as an antiangiogenic compound for treating neovascular diseases such as age-related macular degeneration (AMD).[5−10] The molecular mechanism of action in these biological effects is still unknown. A better understanding of the mechanism of action of AA may lead to improved compound characteristics or an entirely novel target based on the affected signaling pathway.

AA is a cortisene analogue of cortisol (Figure 1a) devoid of anti-inflammatory and immunosuppressive properties.[11] AA is deacetylated in ocular tissue to the active metabolite anecortave desacetate (AdesA).[12] In order to understand the mechanism of action of AA and improve upon its IOP-lowering characteristics, we undertook a yeast three-hybrid (Y3H) screen to identify its cellular binding partner in human trabecular meshwork (TM) cells. TM is the tissue in the anterior chamber of the eye that controls the outflow of aqueous humor, which regulates IOP, and is compromised in glaucoma (Figure 1b).

The Y3H system is a promising alternative to *in vitro* methods traditionally used to identify the protein targets of small molecules, such as affinity chromatography and radiolabeling[13,14] (Figure 1c). An extension of the two-hybrid assay,[15] the Y3H assay is an *in vivo* transcription assay used for the detection of drug−protein target interactions.[16] The methotrexate (Mtx)-anchored Y3H system specifically utilized here is composed of three components: a yeast reporter strain containing a LexA DNA-binding domain (DBD)-responsive HIS3 auxotrophic marker, a "hook" plasmid encoding a fusion of *E. coli* LexA and *E. coli* dihydrofolate reductase (DHFR), and a "fish" plasmid encoding a fusion of the yeast Gal4 activation domain (AD) and a cDNA library of clones encoding candidate ligand binding proteins (Figure 1c). The yeast is transformed with hook and fish plasmids, from which the LexA-DHFR "bait", which binds to Mtx, and Gal4AD-target prey are expressed, respectively. The "bait" is a chimeric molecule, or chemical inducer of dimerization (CID), consisting of Mtx linked here to a drug candidate. Interaction of a potential binding protein with the drug is detected through reconstitution of the DBD and AD of the fish and hook, resulting in transcriptional activation of the HIS3 reporter gene, which allows isolation of yeast clones by growth selection on medium lacking the amino acid histidine with subsequent identification of the candidate receptor through DNA sequencing. Use of the picomolar interaction between Mtx and DHFR as the anchor has afforded the Y3H system the sensitivity to detect a variety

Received: June 13, 2012
Accepted: December 1, 2012
Published: January 9, 2013

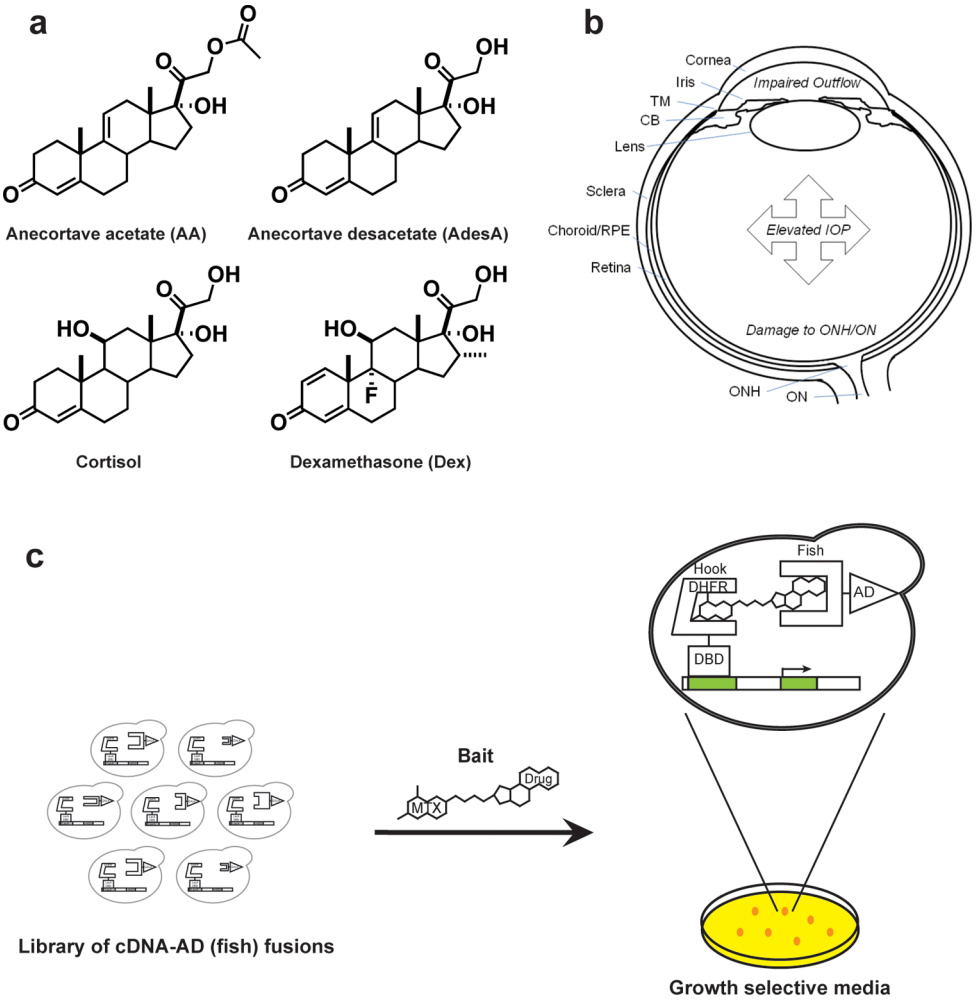

Figure 1. A Y3H screen to identify targets of a glaucoma drug, anecortave acetate. (a) Molecular structure of the drug candidate, anecortave acetate (AA); its active metabolite, anecortave desacetate (AdesA); and related steroids, cortisol and dexamethasone (Dex). (b) Schematic of the human eye and the glaucoma disease process. TM, trabecular meshwork; CB, ciliary body; RPE, retinal pigment epithelium; ONH, optic nerve head; ON, optic nerve; IOP, intraocular pressure. (c) Illustration of the methotrexate (Mtx)-anchored yeast three-hybrid (Y3H) platform. The Y3H system couples drug–protein interactions to transcription activation of a reporter gene. A hybrid ligand of a drug with an anchor moiety (Mtx) can bridge two protein chimeras, the hook and the fish, if the drug interacts with the cDNA encoded-protein of the fish. Positive hook–bait–fish interactions result in the reconstitution of a DNA binding (DBD) and activation (AD) domain of a transcriptional activator and can be detected and isolated by expression of a reporter gene through growth selection from a library of cDNA-AD fish clones. In the Mtx-anchored Y3H system, dihydrofolate reductase (DHFR) and Mtx serve as the anchor connecting the hook and bait.

of small molecule-protein interactions,[17,18] including targets of kinase inhibitors with high nanomolar to low micromolar affinities.[19,20] Surprisingly, given the promise the methotrexate-anchored Y3H system has shown, the Y3H assay is not yet routinely utilized for drug target identification.

In this study, we adapted a state-of-the-art Y2H platform[21,22] to perform a high-throughput Y3H screen, which resulted in the identification of PDE6D (phosphodiesterase-6-delta; prenyl binding protein, PrBP) as an AA-binding protein in human TM cells. PDE6D meets four criteria expected of the molecular target of AA: it specifically binds AA; it is present in the cell cytoplasm where it can interact with plasma membrane-permeable AA; it is expressed in the TM; and overexpression elicits ocular hypertension in the mouse, which is reversed by topical ocular treatment with either AA or AdesA.

RESULTS AND DISCUSSION

Design, Synthesis, and Validation of CIDs ("bait"). The experimental CIDs A1-Mtx, A2-Mtx, D1-Mtx, and D2-Mtx were prepared from AdesA and dexamethasone (Dex) (Figure 1a) via carboxylic acids A1, A2, D1, and D2 (Figure 2). These intermediates were joined to Mtx through a 1,10-diaminodecane linker.[23,24] These chemical modifications do not disrupt receptor binding of either Dex or Mtx.[17] To verify that A1-Mtx is cell permeable, we tested it in a competition experiment with a positive control strain and showed that it could compete the Y3H interaction of D1-Mtx (data not shown).

Y3H Assay Readily Detects Control Dex–GR Interaction. First, we verified that the Y2H screening platform could be adapted for the Y3H assay by identifying the glucocorticoid receptor (GR) from a human normalized universal cDNA library using a CID of Dex and Mtx (D1-Mtx). The yeast reporter strain was transformed with the LexA-DHFR hook vector and the cDNA library and plated on selective medium lacking the amino acids tryptophan and leucine (to select for the hook and fish components of the system) and histidine (to select for yeast cells where a CID-receptor interaction resulted in activation of the HIS3 reporter

dx.doi.org/10.1021/cb300296m | ACS Chem. Biol. 2013, 8, 549–558

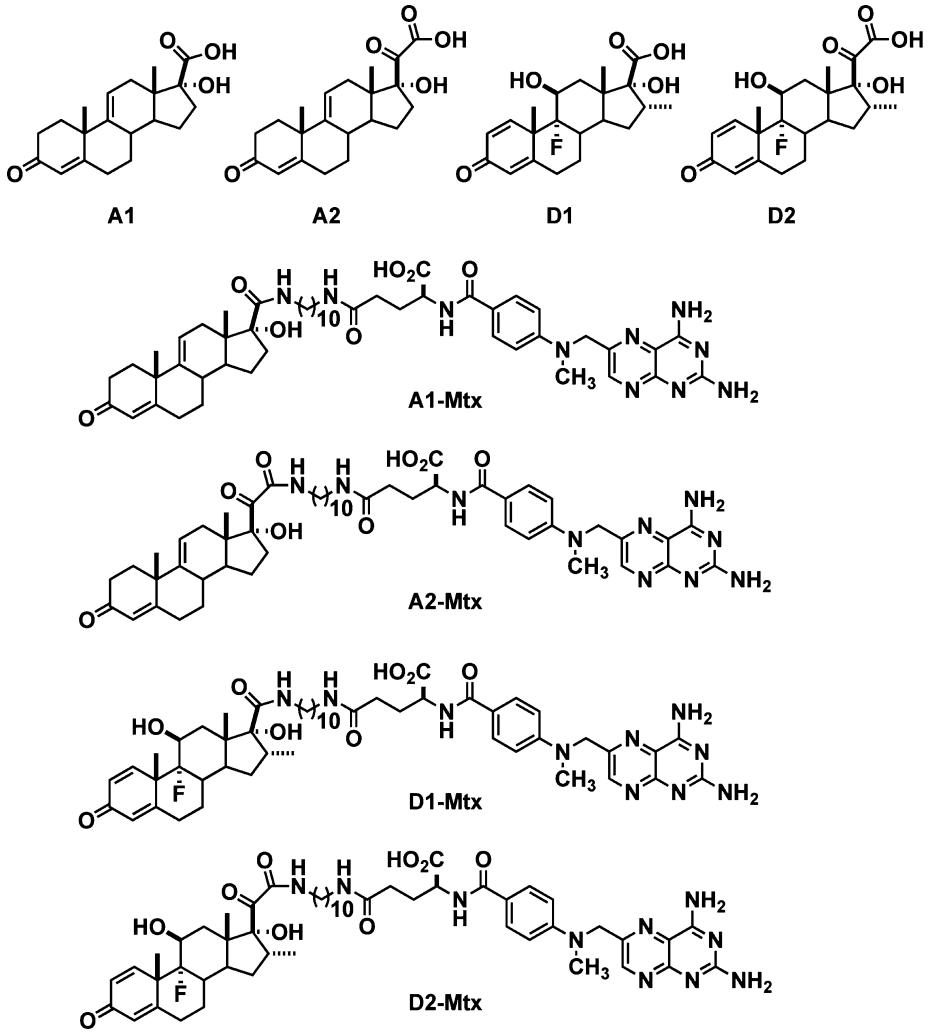

Figure 2. Molecular structures of synthetic intermediates and Y3H CIDs. Structural derivatives of anecortave acetate (A1 and A2) and dexamethasone (D1 and D2) were used as synthetic intermediates for the synthesis of Y3H chemical inducers of dimerization (CIDs) A1-Mtx and A2-Mtx and control CIDs D1-Mtx and D2-Mtx.

gene). The D1-Mtx CID was included in the selective plates to ensure uptake by the yeast cells. Amino-1,2,4-triazole (3-AT), a competitive inhibitor for the product of the HIS3 reporter gene, was also added to the medium to increase the stringency of the selection. After 7 days of growth on selective medium, a total of 96 clones harboring potential interactors of the D1-Mtx CID were picked and analyzed further (Figure 3a).

In a secondary liquid growth assay, these clones were grown in selective medium with and without D1-Mtx for 6 days. A calculated ratio of the $OD_{\text{with compound}}$:$OD_{\text{without compound}}$ was used to select candidate hit clones by comparison with a positive control strain containing a prey vector with the rat GR and a negative control with an empty prey vector (Figure 3b). Nine clones with growth ratios greater than that of the positive control were isolated, retransformed into yeast, and again tested for D1-Mtx-dependent growth over time. Six of the nine secondary hits grew independently of the presence of D1-Mtx and were eliminated as false positives, while three grew in a D1-Mtx-dependent fashion and were deemed to be real interactions (Figure 3c).

To confirm that our selection criteria identified genuine hits, fifty of the clones from the original screen were sequenced. Of these clones, only the three that displayed selective growth in the presence of D1-Mtx corresponded to the human GR. All other clones were D1-Mtx-independent (false positives) or did not display growth after retransformation (negative clones). Together these data established that we had a robust experimental framework to readily isolate true protein−drug interactions and eliminate false positives and negative clones using our Y3H screen.

Y3H Screen for AA Binding Targets. The screen for AA binding targets was performed using a custom-made cDNA library constructed from immortalized human glaucomatous TM (GTM3 or HTM3) cells, a TM cell line[25] that is a conceptually relevant source of targets for AA in affecting glaucoma pathophysiology. In the primary screen of the CID A1-Mtx, clones were picked and subsequently passaged three times in selective medium to more efficiently exclude negative clones. After successive passages, a primary hit pool of 190 clones was evaluated in a secondary liquid growth assay (Figure 4a). Every clone that grew in selective medium in the absence of A1-Mtx was discarded as a false positive. The remaining 62 clones that passed the secondary screen threshold were then analyzed by sequencing, revealing 24 potential protein binders. Interestingly, only two clones, ID60 and ID30, were represented multiple times in the hit list while the remaining

dx.doi.org/10.1021/cb300296m | ACS Chem. Biol. 2013, 8, 549−558

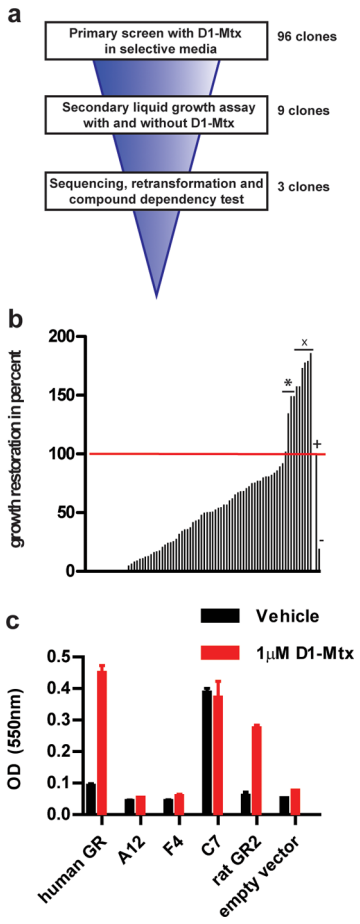

Figure 3. Validation of Y3H screening platform. (a) Selection funnel illustrating the screening steps that enabled the isolation of three true hit clones and the attrition of false positives in the Y3H screen of D1-Mtx. (b) Secondary liquid growth assay used to determine growth dependence of primary screen hits on the D1-Mtx CID in comparison with the (+) positive control rat glucocorticoid receptor (rat GR2, 100%) and (−) negative control (empty vector, 20%). Of the nine clones that exhibited growth dependence greater than that of the positive control, six were discovered to be (x) false positives in the subsequent retransformation and compound-dependency test, and three clones that remained compound-dependent corresponded to the (*) human GR. (c) Growth of selected clones in the presence of 1 μM D1-Mtx CID or vehicle control after retransformation. Only a clone corresponding to the human glucocorticoid receptor (human GR) exhibited compound-dependent growth, while C7, a false positive clone, did not. Negative clones A12 and F4 did not exhibit growth in comparison with the positive (rat GR2) and negative (empty vector) controls and were deemed negative clones.

hits were singletons. Thus, these two candidate targets along with two singletons of biological interest, ID7 and ID45, underwent further validation steps. Many of the remaining clones were discounted as known Y2H artifacts.

The four selected clones were isolated, retransformed, and tested for growth with and without A1-Mtx to confirm CID dependence. Yeast transformed with ID60, ID30, ID7, or ID45 were capable of growth under nonselective conditions, indicating that the clones were nontoxic to yeast (Supplementary Figure 1), but as expected showed no growth under selective conditions in the presence of DMSO or 10 μM D1-Mtx (Figure 4b). Selective growth of ID60 did occur in the presence of 1 μM A1-Mtx, whereas both ID30 and ID60 grew in the presence of 10 μM A1-Mtx, suggesting that ID60 had a stronger interaction with A1-Mtx than ID30 (Figure 4b).

Next, we evaluated the CID A2-Mtx for growth selectivity in the yeast liquid growth assay. Growth under positive and negative growth conditions verified the fidelity of the system (Supplementary Figure 2). Selective growth of ID60 and ID30 was observed with 10 μM A2-Mtx, but not with the corresponding control CID D2-Mtx (Figure 4c). These results parallel those seen with A1-Mtx/D1-Mtx, but within an earlier time of growth onset: ID60 reached an $OD_{550\ nm}$ of 0.5 after 24 h *vs* 48 h, while ID30 interaction was detected by 48 h *vs* 72 h. This suggests that the extended linkage in A2-Mtx provides more optimal coupling of the Y3H complex and provides further support for the specificity of the Y3H interactions. In our previous work, we had characterized the effect of linker length in the CID on the Y3H signal and found an extension of 3−5 carbons enabled detection of transcription in the Y3H assay at lower CID concentrations and earlier time points.[18] Additionally, there is a possibility that the additional carbonyl group in the A2-Mtx CID mimics the interaction between the hydroxyl group in AdesA and the target protein. By contrast, more robust growth was evident in control assays with rGR2 and D1-Mtx than with D2-Mtx, suggesting that the shorter linkage is more optimal for this Y3H complex (Supplementary Figure 3).

In principle, the more abundant a hit, the more likely that it is a true interactor. Thus, our initial testing indicated that our assumption to discount singleton hits was reasonable. However, the relative abundance of the starting mRNA transcripts in the cDNA library and the strength of the Y3H interaction may affect the hit abundance. To further investigate this, 15 additional singleton hits, excluding those that are commonly found false positives identified in Y2H screens and catalogued in the Dualsystems Biotech false positive database were selected from the secondary screen list for retransformation analysis. None of the 15 clones showed consistent, reproducible growth in the presence of A1-Mtx or A2-Mtx (data not shown).

Sequence analysis of the clones corresponding to ID60 and ID30 revealed that both encoded a full-length ORF; however, all 36 clones of ID30 were out-of-frame (+1 reading frame) with respect to the upstream GAL4 AD, a commonly found occurrence in Y2H screens. Many out-of-frame clones that code for short hydrophobic peptides with no sequence homology to known proteins can appear to bind specifically with the bait.[26] Out-of-frame clones can also be real interactions in a Y2H/Y3H system due to in-frame protein production as the cell adapts by "ribosome sliding" to prevent production of an out-of-frame protein.[27] To examine this further, we cloned ID30 in-frame with the GAL4 AD and tested for growth in selective media in the presence and absence of A1-Mtx. Expression of in-frame ID30 failed to result in CID-dependent growth in yeast but did support growth in control SD-TL growth media (Supplementary Figure 4), suggesting that in-frame ID30 was not toxic to yeast and that the original out-of-frame ID30 was a false positive. Utilizing our Y3H screening strategy we narrowed the field of *candidate targets to one final hit, ID60 or phosphodiesterase 6D (PDE6D).* PDE6D is part of the PDE6 phototransduction system and a known prenyl binding protein (alias PrBP).

In order to assess the specificity of the interaction between A1-Mtx and PDE6D, a Y3H-based competition assay was carried out. Yeast expressing the LexA-DHFR hook and the PDE6D prey were loaded either with A1-Mtx alone or with A1-

dx.doi.org/10.1021/cb300296m | *ACS Chem. Biol.* 2013, 8, 549−558

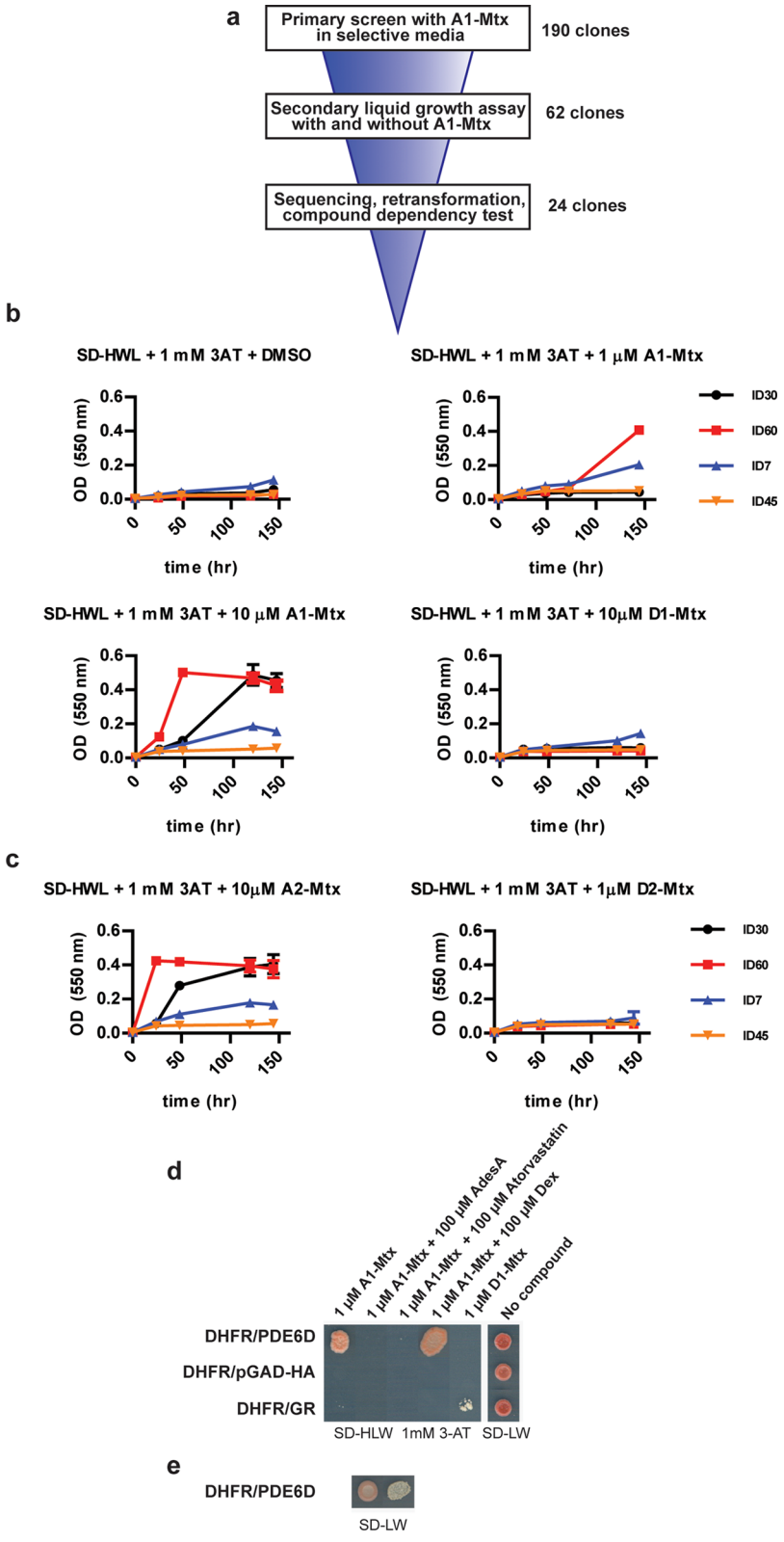

Figure 4. Y3H screen with A1-Mtx identifies PDE6D as an AA-interacting protein. (a) Selection funnel illustrating the screening steps that enabled the identification of phosphodiesterase 6-delta (PDE6D) as an AA-binding protein and the attrition of false positives in the Y3H screen of A1-Mtx. (b) Growth of selected clones in the presence of 1 μM, 10 μM A1-Mtx CID, 10 μM D1-Mtx, or vehicle control after retransformation. Optical density ($OD_{550\ nm}$) was determined over time. The ID60 (PDE6D) clone grew in the presence of 1 μM A1-Mtx, whereas both ID30 and ID60 clones exhibited growth at 10 μM A1-Mtx, suggesting that ID60 had a stronger interaction with A1-Mtx compared to ID30. Two additional clones of biological interest (ID7, ID45) did not exhibit compound-dependent growth after retransformation, nor did any of the clones show growth in the presence of 10 μM D1-Mtx. (c) Growth of selected clones in the presence of 10 μM A2-Mtx CID or 1 μM D2-Mtx after retransformation. Optical density ($OD_{550\ nm}$) was determined over time. Selective growth of ID60 (PDE6D) and ID30 was also observed with 10 μM A2-Mtx (which possessed a longer linker length than A1-Mtx) but within an earlier time of growth onset, suggesting that the extended linkage was more favorable in

dx.doi.org/10.1021/cb300296m | ACS Chem. Biol. 2013, 8, 549−558

Figure 4. continued

forming the Y3H complex. Controls with 1 μM D2-Mtx with a similar length linker did not produce compound-dependent growth. (d) Competition of A1-Mtx interaction with free AdesA and atorvastatin in the Y3H assay. Cells expressing the indicated hook−prey combinations were spotted onto selective medium supplemented with A1-Mtx and the free compounds AdesA, atorvastatin, and dexamethasone (Dex). As a control, the interaction between D1-Mtx and GR was used. Both AdesA and atorvastatin are able to compete out the interaction of A1-Mtx with PDE6D, whereas the control molecule dexamethasone has no effect on the interaction. (e) Neither AdesA nor atorvastatin show any toxicity for the cells on nonselective medium.

Mtx in the presence of excess free AdesA or atorvastatin (Figure 4d). Atorvastatin is another known ligand of PDE6D that has also been detected in a Y3H screen.[28] Cells were spotted onto solid selective medium (SD-HLW + 1 mM 3-AT) or onto nonselective medium (SD-LW) as a control. Both free AdesA and atorvastatin were able to compete out the interaction between A1-Mtx and PDE6D, whereas the control compound dexamethasone had no discernible effect on the interaction. Neither free AdesA nor atorvastatin were toxic, since the cells were able to grow on nonselective medium in the presence of both compounds (Figure 4e). Competition assays were also performed with ID30, ID7, and ID45, and AdesA was only able to compete out the interaction between A1-Mtx and ID30 (Supplementary Figure 5).

***In Vitro* Validation of Target: AdesA Binds to PDE6D.** Next, we proceeded to characterize the interaction of AdesA with PDE6D *in vitro*. Pulldown assays were performed with purified His-tagged DHFR and streptavidin-tagged PDE6D incubated with or without A1-Mtx (50 μM) and purified over a StrepTactin resin. Eluates were then analyzed by Western blotting with an anti-His antibody to detect the presence of isolated DHFR. Incubation in the presence of A1-Mtx revealed a band corresponding to the size of the His-tagged DHFR (~20 kD), which could be competed off in elutions incubated with excess AdesA (500 μM) (Figure 5). His-DHFR detected in the elution fractions of AdesA competed with A1-Mtx as observed in the three elution steps.

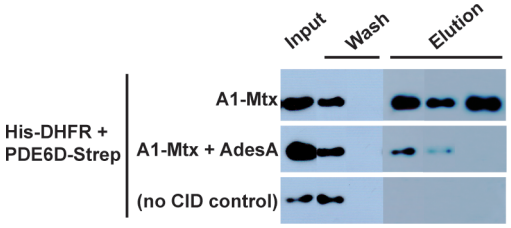

Figure 5. *In vitro* analysis of PDE6D interaction with A1-Mtx CID. Strep-tagged PDE6D and His-tagged DHFR were mixed with or without 500 μM AdesA (Drug) and with or without 50 μM A1-Mtx (Drug conjugate) and purified over a StrepTactin resin. His-tagged DHFR was only observed in pull-down eluates in the presence of A1-Mtx and not in the absence of the CID. Further incubation with 10X AdesA abrogated the *in vitro* interaction of A1-Mtx with DHFR as measured by its decrease in the eluate. The first and second "Wash" lanes correspond to the first and fifth washes, respectively. The three "Elution" lanes correspond to three sequential elutions that were performed.

Additionally we deployed surface plasmon resonance (SPR) to quantitate the interaction of A1-Mtx captured on DHFR with free PDE6D. Atorvastatin was used as a positive binding control. A CID of atorvastatin and Mtx (atorvastatin-$(EG)_6$-Methotrexate) captured on DHFR was found to interact with PDE6D with a K_d of 58 nM, in good agreement with the reported value of 65 nM for atorvastatin binding PDE6D [28] (*data not shown*). SPR analysis with A1-Mtx resulted in a K_d in the low micromolar range (~2.7 μM) (Supplementary Figure 6). Interestingly, PDE6D binds geranylgeranyl and farnesyl moieties of PDE6 subunits PDE6A and PDE6B with K_d's of 19.06 and 0.70 μM, respectively.[29]

***In Vivo* Validation of Target: PDE6D Overexpression Elevates Intraocular Pressure.** Finally we developed a mouse model to investigate the effect on IOP of PDE6D with AA or AdesA. Mice were injected intravitreally with an adenovirus containing a CMV promoter driving expression of PDE6D (Ad.PDE6D). Appropriate anterior segment expression of adenoviral expressed genes has been previously demonstrated, and adenoviral infection of various control vectors is not found to have any effect on IOP.[30−32] We confirmed overexpression of PDE6D with the adenoviral vector in TM cells by Western blot (Figure 6a) and observed a time-dependent increase in IOP following overexpression of PDE6D in the mice (Figure 6b). Ad.PDE6D-injected mice were treated with either vehicle or drug on days 12−14 (Figure 6c) or days 40−42 (Figure 6d) postinjection, and IOP was measured periodically over the course of the 43-day study. Topical ocular dosing of ocular hypertensive eyes with AA significantly lowered IOP relative to vehicle on days 13 and 14 (Figure 6c). Both atorvastatin (a statin with known PDE6D-binding activity) and Xalatan (a uveoscleral outflow enhancing glaucoma drug) were used as positive controls and tended to lower IOP beyond vehicle (negative control) but did not reach statistical significance. Rosuvastatin, another member of the statin drug family, but which does not bind PDE6D[28] and should therefore function as a negative control, was statistically indistinguishable from vehicle. Topical ocular dosing with either AA or AdesA over days 40−42 resulted in significant IOP lowering with AdesA equivalent to Xalatan and superior to AA (Figure 6d). No statistically significant IOP effects of the test agents were noted on the contralateral, uninjected eyes in either dosing period.

Conclusions. Using a Y3H approach to search for the molecular binding partner of AA, we identified phosphodiesterase 6D (PDE6D) as the target binding protein in human TM cells. PDE6 is located in the rod and cone photoreceptors and is composed of PDE6A and PDE6B catalytic subunits, a PDE6G inhibitory subunit, and a PDE6D regulatory subunit. PDE6D is known to reduce activation of retinal rod photoreceptor PDE6; however, PDE6D itself lacks phosphodiesterase activity.[33] PDE6D is also known to be a ubiquitous prenyl-binding protein (PrBP) that interacts with numerous prenylated proteins at their farnesylated (*e.g.*, PDE6B) or geranylgeranylated (*e.g.*, PDE6A) C-termini.[33] Deletion of *Pde6d* in mice results in viable, fertile mice with normal retinal development but with impaired transport of prenylated GRK1 and PDE in photoreceptors.[34] Our SPR binding data supports AA binding directly to PDE6D and functional data from our mouse Ad.PDE6D model indicates that AA is capable of

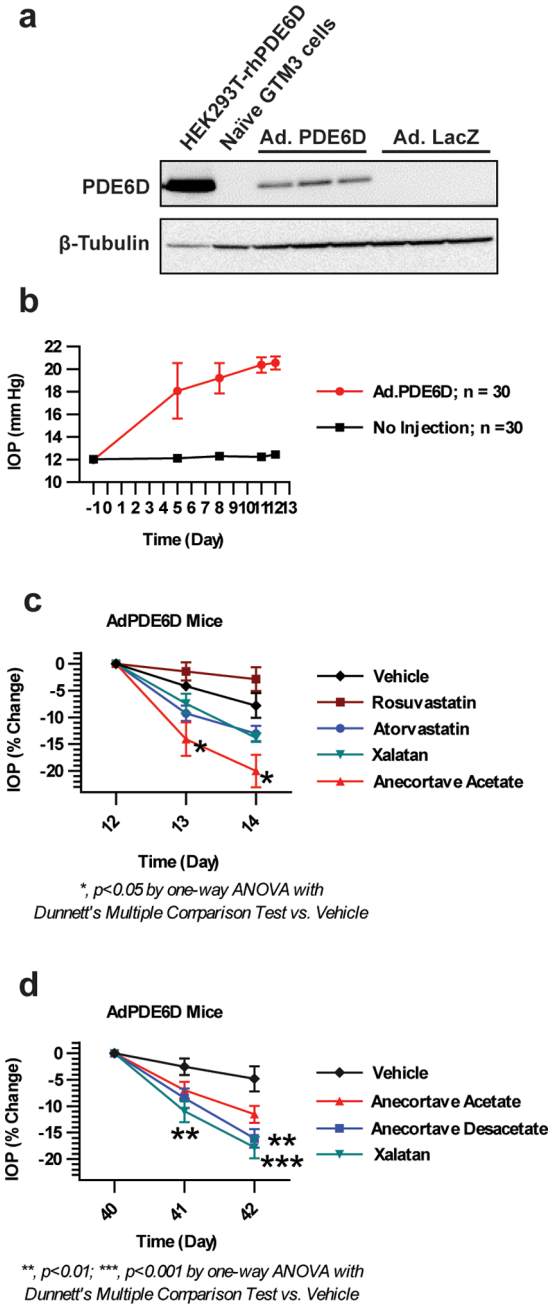

Figure 6. PDE6D overexpression elevates intraocular pressure in a mouse IOP model. (a) Western blot analysis of the production of PDE6D (~17 kDa) from GTM3 cells transduced with Ad.PDE6D. Controls include purified recombinant PDE6D from HEK293T cells, naïve GTM3 cells, and GTM3 cells transduced with Ad.LacZ. β-Tubulin (~50 kDa) staining was used to show equivalent protein loading for GTM3 cell lysates. Ad.PDE6D and Ad.LacZ samples were from triplicate transductions. (b) Mouse eyes were injected intravitreally on day 0 with an adenovirus expressing PDE6D (Ad.PDE6D), and IOP was measured over time. The eyes of Ad.PDE6D-injected mice were topically treated with either vehicle or drug on (c) days 12–14 or (d) days 40–42 postinjection. All drugs were formulated as 1% (w/v) ophthalmic suspensions. For 12 days after injection of the adenovirus, PDE6D overexpression was observed to cause a time-dependent increase in IOP. Upon dosing of eyes with AA or AdesA, IOP was significantly reduced relative to vehicle-treated eyes during observation over the following 2 days. Glaucoma standard of care drugs typically lower IOP by 20–30% in animal models and in humans. Both atorvastatin (a known PDE6D-interacting drug) and Xalatan (a positive control) also lowered IOP beyond vehicle treatment but did not reach statistical significance. Rosuvastatin, another member of the statin drug family that does not bind PDE6D, was statistically indistinguishable from the vehicle. These data indicate that PDE6D overexpression can cause ocular hypertension, which can be reversed by topical ocular treatment with either AA or AdesA.

reversing the Ad.PDE6D-mediated IOP elevation. The mechanism of action for this effect is unknown. It is known that the Rho family of G-proteins require prenylation in order to regulate actin cytoskeleton contraction and that the Rho kinase/Rho GTPase pathway may modulate aqueous humor outflow in the eye.[35] Angiogenesis may also be inhibited by blocking the geranylgeranylation of RhoA with HMG-CoA reductase inhibitors (statins).[36] We speculate that overexpression of PDE6D in the anterior segment of the eye, as exampled in our mouse Ad.PDE6D model, may modulate transport of prenylated proteins, particularly members of the Rho family, resulting in altered TM physiology with a phenotype of elevated intraocular pressure.

PDE6D has several other interesting aspects to its physiology. In addition to the prenylated PDE6A and PDE6B proteins, PDE6D has been shown to interact with non-prenylated proteins including Rac, Rab13, H-Ras, Rap, Rho6, Ar12-GTP, RPGR, and GRK1/7.[29,33,37,38] PDE6D can also directly interact with the PDE5 inhibitor PF-4540124.[39] The vasodilator prostacyclin exerts its effects through the G protein-coupled receptor IP, and PDE6D has been shown to interact with IP and affect IP recycling.[40] Prostacyclin and IP receptor analogues have been shown to have IOP lowering activity.[41] In a recent report, PDE6D expression was found to be downregulated in idiopathic pulmonary fibrosis lungs and affect the proliferation rate of alveolar epithelial cells.[42]

In our binding studies, we showed that AA can interact with PDE6D with a K_d in the low micromolar range (~2.7 μM). Interestingly, PDE6D binds geranylgeranyl and farnesyl moieties of PDE6 subunits PDE6A and PDE6B with K_d's of 19.06 and 0.70 μM, respectively.[29] The other PDE6D binding molecule, atorvastatin, was found to interact with PDE6D with a K_d of 58 nM. Atorvastatin had been shown to interact with PDE6D with a K_d of 65 nM[28] and may inhibit neovascularization independent of HMG-CoA-reductase inhibition.[43] This suggests that small molecule binding to PDE6D may play a role in antiangiogenesis and explain the antiangiogenic effect of AA.

In our present studies, it is unclear if PDE6D is also the target of AA in antiangiogenesis because we used a glaucoma TM cell-derived cDNA library to identify PDE6D. TM cells are the target tissue that controls aqueous humor outflow and IOP in the eye; therefore we focused our investigations on the IOP and not the angiogenesis aspects of PDE6D. However, it is interesting to note that the PDE6D-binding statin, atorvastatin, can inhibit laser-induced choroidal neovascularization in mice.[44] Other statins can also be antiangiogenic, so atorvastatin may not have unique properties in this regard. It is difficult to distinguish the normal statin effects on protein isoprenylation from potential PDE6D-mediated effects on prenyl binding. It would be of interest to evaluate IOP levels in *Pde6d*−/− mice[34] and investigate whether they have diminished laser-induced choroidal neovascularization.

dx.doi.org/10.1021/cb300296m | ACS Chem. Biol. 2013, 8, 549–558

Finally, this study provides perhaps the most compelling published evidence for the efficacy of the methotrexate-anchored Y3H system in identifying the molecular targets of drugs and lead compounds. Identification of the biological target of a drug, both the target that produces the beneficial effect and off targets that lead to side effects, continues to be a hurdle in the drug discovery process. Target identification efforts mainly rely on traditional methods such as affinity chromatography that are labor intensive and prone to artifacts. The Y3H assay was initially proposed as a modern alternative to these methods that utilized the power of genomics,[14,16] providing advantages such as overexpression of all candidate genes and straightforward hit identification by sequencing. However, the original Y3H assay was not sufficiently sensitive and was reputed to be unable to detect the micromolar interactions typical of lead compounds. With our introduction of the picomolar interaction between Mtx and DHFR as the anchor in the Y3H assay, the sensitivity of the assay was significantly increased, and there are now published reports demonstrating that the methotrexate-anchored Y3H assay can detect interactions up to low micromolar affinity and potentially discover new targets of known drugs. This is the first report, to our knowledge, of a study that identifies a new molecular target of a drug using a Y3H screen and validates that molecular target all the way from quantitative *in vitro* measurements to an animal model of the disease.

In summary, we have identified PDE6D as the cellular target of AA that modulates IOP in the eye. Future work may involve a search for more potent low molecular weight modulators of PDE6D activity and/or modulators of the pathways affected by PDE6D. Such molecules may be used to improve upon the IOP-lowering activity of AA noted previously in glaucoma patients, in particular steroid-induced glaucoma patients, in the clinic. However, attention must be paid to the potential untoward effects on the retinal phototransduction pathway that may be incurred by targeting PDE6D for IOP-lowering purposes. Determining if PDE6D has a role in angiogenesis inhibition will also be of interest in future studies.

METHODS

Chemical Inducer of Dimerization (CID) Synthesis. Dexamethasone (Dex) was converted to acid D1 by reaction with periodic acid and to keto acid D2 by reaction with air/Cu(II) followed by $NaClO_2$.[45] Anecortave desacetate (AdesA) was subjected to comparable reaction conditions to afford acid A1 and keto acid A2. The CIDs were assembled using Aldrich compounds D14204, 858269, and 861553 under conditions adapted from published syntheses[23] (see Supporting Information, chemical synthesis and analysis). All compounds were dissolved in either 100% DMSO or 100% DMF to a final stock concentration of 100 mM for yeast studies. The A1-Mtx CID was shown to be nontoxic to yeast cell growth at CID concentrations up to 100 μM (Supplementary Figure 7).

Plasmids. The *E. coli* dihydrofolate reductase-encoding gene (eDHFR) was generated by PCR amplification of plasmid pLL-1 (Active Motif, Carlsbad, CA) using primers F, CTCGAGCTCGCCACCATGGTGGGTTCT and R, GACCGTCGACTTACCGCCGCTCCAGAAT. The 519-bp PCR product was digested with Sac1 and Sal1 and subcloned into pLexA-N vector (Dualsystems, Schlieren, Switzerland) resulting in vector pLexA-N.eDHFR encoding a LexA-$(GlySerGly)_2$-eDHFR fusion protein.

The rat glucocorticoid receptor (GR) hormone binding domain cDNA encoding F620S and C656G mutations[24,46] was synthesized (Blue Heron Biotechnology) with Sfi1 restriction sites on 5′ and 3′ termini to facilitate subcloning into the pGAD-HA vector (Dualsystems), resulting in vector pGAD-HA-rGR2 encoding a GAL4 AD-$(GlySerGly)_2$-rGR2 fusion protein.

Hook and fish vectors were generated with $(Gly\text{-}Ser\text{-}Gly)_2$ linkers to allow for the two domains of the protein chimera to function properly.[18,47] To ensure that the constructed hook and fish vectors are correctly expressed in yeast, immunoblotting of cell extracts was performed using a mouse monoclonal antibody directed against the LexA domain (Santa Cruz, Santa Cruz, California). Robust expression of both the hook and fish gene products was detected (Supplementary Figure 8).

Strains. The yeast reporter strain NMY51-C3 has been previously described and was constructed by Chidley *et al.* by knocking out PDR5 and SNQ2 from a parental strain, NMY51, prepared by Dualsystems.[28] NMY51-C3 is auxotrophic for histidine, adenine, uracil, leucine, and tryptophan and carries three LexA-responsive reporter genes: HIS3, ADE2, and lacZ. The genotype of NMY51-C3 is MATa his3Δ200 trp1-901 leu2-3,112 ade2 LYS2::(lexAop)4-HIS3 ura3::(lexAop)8-lacZ (lexAop)8-ADE2 GAL4 Δpdr5 Δsnq2.

Pairwise Y3H Interaction Assays. To test the feasibility of the Y3H approach, pairwise combinations of hook vectors pLexA-eDHFR or control pLexA-laminC and fish vector pGAD-HA-rGR2 were transformed into yeast. To ensure that the bait does not autonomously activate transcription of the HIS3 reporter gene, a self-activation test was performed. Hook and fish vectors were co-transformed and checked for growth in minimal medium lacking amino acids tryptophan, leucine, and histidine (selective medium) with or without bait (D1-Mtx) (Supplementary Figure 9). Only the triple combination of pLexA-eDHFR, pGAD-HA-rGR2, and D1-Mtx on SD-HLW media was active, confirming that there is no autonomous activation within the system. A very strong interaction would be required to observe activity on SD-AHLW plates.

cDNA Libraries and Screening. The human normalized universal cDNA library was purchased from Takara (Mountain View, CA, USA).

A custom cDNA library was constructed in the pGAD-HA vector from oligo dT-primed total RNA derived from human GTM3 cells.[25] cDNA was directionally cloned into the Sfi1 restriction site resulting in TM-encoding GTM3 cell-derived polypeptides fused to the carboxy terminus of $(GlySerGly)_2$ and the GAL4 activation domain. Complexity of the cDNA library was determined to be 1E7 independent clones with an average insert size of 1.1-kb, size range of 0.6- to 10-kb, and 100% containing an insert size greater than 250-bp.

Yeast strain NMY51-C3 was transformed with pLexA-N.eDHFR and the TM cDNA library and screened on selective (SD) medium lacking the amino acids tryptophan, leucine, and histidine and containing 1 mM 3-AT (Sigma, Buchs, Switzerland) and 10 μM AdesA. Transformation efficiency was determined to be 2.34×10^6 clones in total. 190 clones were picked. To dilute out the compound from the primary clones, all clones were grown for 10 days in SD-TL with serial passaging (7 passages total).

Secondary Liquid Growth Assay. Selected clones were inoculated in (1) SD-HTL + 1 mM 3AT and (2) SD-HTL + 1 mM 3AT + 10 μM A1-Mtx. Growth rates under selection were determined over a period of 6 days, and cell densities were measured after 3 and 6 days of growth at 30 °C. Starting OD of cultures was 0.05. The assay was performed in duplicate. To determine the growth stimulation score (GSS), growth in the presence and absence of A1-Mtx was compared. A GSS of 1 means no difference in growth in the presence or absence of compound.

Pull-down Assay. In the pull-down assay, the hook scaffold was tagged with His and the fish protein with Strep and expressed in a cell free expression system. Both proteins were mixed with A1-Mtx to a final concentration of 20 μM and purified over a StrepTactin Resin. Flow-through, wash steps (5×), and elution fractions (3×) were analyzed by SDS-PAGE and Western blot using an anti-His antibody.

SPR Analysis of PDE6D−AdesA Interaction. The strength of the PDE6D-AdesA binding interaction was determined with Biacore 2000 analysis (Biaffin GmbH & Co KG, Kassel, Germany). DHFR-His was covalently coupled to flow cells via standard amine coupling. PDE6D (4.7 mg mL^{-1} in 40 mM Tris pH 7.5, 50 mM NaCl, 1 mM EDTA, 1 mM 2-ME, 10% glycerol) was prepared and used to

determine the binding strength with atorvastatin-$(EG)_6$-Methotrexate and AA-$(EG)_6$-Methotrexate. On and off rates were determined. Purified, untagged PDE6D protein was obtained from overexpression in *E. coli*. DHFR was covalently immobilized to CM5 sensor chip followed by (i) qualitative binding with titrated PDE6D in the presence or absence of MTX-derivatives and (ii) quantitative binding with the determination of affinity and rate constant (K_d).

Ad.PDE6D. Ad.PDE6D (4.9E12 vp mL^{-1}; 1.56E11 pfu mL^{-1}; 10% glycerol/PBS buffer) was generated by Vector Biolabs, Inc. (Philadelphia, PA) starting with a plasmid DNA clone for human PDE6D (NM_002601) obtained from Origene Technologies, Inc. (Rockville, MD). This viral vector is a first generation ($\Delta E1/\Delta E3$) adenovirus serotype 5 expressing the PDE6D gene under control of the cytomegalovirus-IE promoter/enhancer.

Western Blot of Ad.PDE6D. Ad.PDE6D or control Ad.LacZ (U Iowa GTVC) vectors were transduced in GTM3 cells at 100 moi, and cell lysates were harvested 48 h later. Proteins were separated by SDS-PAGE and transferred to PVDF membranes for immunostaining with either a 1:500 dilution of rabbit polyclonal anti-PDE6D antibody (Origene cat. no. TA308586) or 1:10,000 dilution of mouse monoclonal anti-β-tubulin antibody (Invitrogen) followed by 1:10,000 dilution of secondary anti-mouse IgG coupled to horseradish peroxidase. Chemiluminescence was performed using GE ECL Prime Western Blotting Detection reagent. Detection of chemiluminescent bands was performed using the Protein Simple FluorChem M detector. Purified human PDE6D derived from HEK392T cells (Origene cat no. TP303172) was used as a positive control.

***In Vivo* Analysis of Ad.PDE6D.** *In vivo* studies were performed essentially as previously described.[30,31] BALB/cJ mice (Jackson Laboratories, Bar Harbor, Maine) were examined at day −1 by direct ophthalmoscopy (hand-held ophthalmoscope, model 11710; Welch-Allyn, Skaneateles Falls, NY) to confirm normal appearance and freedom from signs of ocular disease. At day 0, mice were anesthetized using an anesthesia solution (acepromazine 1.8 mg/kg, ketamine 73 mg/kg, and xylazine 1.8 mg/kg; intraperitoneal injection). A randomly assigned eye of each mouse was then topically anesthetized with 1−2 drops of 0.5% tropicamide (Alcaine; Alcon Laboratories) and given a single intravitreal injection of a suspension of adenovirus (2E7 pfu) in a volume of 2 μL. The uninjected contralateral eye served as a paired control. IOP measurements were taken in conscious mice using the TonoLab rebound tonometer (Helsinki, Finland). The IOP investigator was masked to the identity of the injected adenovirus, to which eye was injected, and to the formulations used.

Formulations. AA, AdesA, atorvastatin, and rosuvastatin were prepared as 1% (w/v) ophthalmic suspension formulations for topical ocular application.

■ ASSOCIATED CONTENT

Ⓢ Supporting Information

This material is available free of charge via the Internet.

■ AUTHOR INFORMATION

Corresponding Author

*E-mail: (A.R.S.) allan.shepard@novartis.com; (V.W.C.) vc114@columbia.edu.

Notes

The authors declare the following competing financial interest(s): Columbia University is the assignee of U.S. Patent 7,419,780 on the Methotrexate Yeast 3-Hybrid Technology, which will be developed by HybrID Drug Discovery, LLC of La Jolla, California. V.W.C. will be the Chief Scientific Officer and a Member of HybrID Drug Discovery, LLC.

■ ACKNOWLEDGMENTS

We acknowledge B. Zimmermann and colleagues at Biaffin GmbH & Co. KG for the surface plasmon resonance work, AMRI for CID synthesis, and J.C. Millar for help with the *in vivo* analysis of Ad.PDE6D. This study was wholly supported by Alcon Research, Ltd.

■ REFERENCES

(1) Candia, O. A., Gerometta, R., Millar, J. C., and Podos, S. M. (2010) Suppression of corticosteroid-induced ocular hypertension in sheep by anecortave. *Arch. Ophthalmol. 128*, 338−343.

(2) Prata, T. S., Tavares, I. M., Mello, P. A., Tamura, C., Lima, V. C., and Belfort, R. (2010) Hypotensive effect of juxtascleral administration of anecortave acetate in different types of glaucoma. *J. Glaucoma 19*, 488−492.

(3) Robin, A. L., Clark, A. F., Covert, D. W., Krueger, S., Bergamini, M. V., Landry, T. A., Dickerson, J. E., Scheib, S. A., Realini, T., Defaller, J. M., and Cagle, G. D. (2009) Anterior juxtascleral delivery of anecortave acetate in eyes with primary open-angle glaucoma: a pilot investigation. *Am J Ophthalmol 147*, 45−50.e2.

(4) Robin, A. L., Suan, E. P., Sjaarda, R. N., Callanan, D. G., and Defaller, J. (2009) Reduction of intraocular pressure with anecortave acetate in eyes with ocular steroid injection-related glaucoma. *Arch. Ophthalmol. 127*, 173−178.

(5) Augustin, A. (2006) Anecortave acetate in the treatment of age-related macular degeneration. *Clin Interv Aging 1*, 237−246.

(6) D'Amico, D. J., Goldberg, M. F., Hudson, H., Jerdan, J. A., Krueger, D. S., Luna, S. P., Robertson, S. M., Russell, S., Singerman, L., Slakter, J. S., Yannuzzi, L., and Zilliox, P. (2003) Anecortave acetate as monotherapy for treatment of subfoveal neovascularization in age-related macular degeneration: twelve-month clinical outcomes. *Ophthalmology 110*, 2372−2383 ; discussion 2384−2385.

(7) D'Amico, D. J., Goldberg, M. F., Hudson, H., Jerdan, J. A., Krueger, S., Luna, S., Robertson, S. M., Russell, S., Singerman, L., Slakter, J. S., Sullivan, E. K., Yannuzzi, L., and Zilliox, P. (2003) Anecortave acetate as monotherapy for the treatment of subfoveal lesions in patients with exudative age-related macular degeneration (AMD): interim (month 6) analysis of clinical safety and efficacy. *Retina 23*, 14−23.

(8) Klais, C. M., Eandi, C. M., Ober, M. D., Sorenson, J. A., Sadeghi, S. N., Freund, K. B., Spaide, R. F., Slakter, J. S., and Yannuzzi, L. A. (2006) Anecortave acetate treatment for retinal angiomatous proliferation: a pilot study. *Retina 26*, 773−779.

(9) Russell, S. R., Hudson, H. L., and Jerdan, J. A. (2007) Anecortave acetate for the treatment of exudative age-related macular degeneration–a review of clinical outcomes. *Surv. Ophthalmol. 52* (Suppl 1), S79−90.

(10) Schmidt-Erfurth, U., Michels, S., Michels, R., and Aue, A. (2005) Anecortave acetate for the treatment of subfoveal choroidal neovascularization secondary to age-related macular degeneration. *Eur. J. Ophthalmol. 15*, 482−485.

(11) Clark, A. F. (2007) Mechanism of action of the angiostatic cortisene anecortave acetate. *Surv. Ophthalmol. 52* (Suppl 1), S26−34.

(12) Missel, P., Chastain, J., Mitra, A., Kompella, U., Kansara, V., Duvvuri, S., Amrite, A., and Cheruvu, N. (2010) In vitro transport and partitioning of AL-4940, active metabolite of angiostatic agent anecortave acetate, in ocular tissues of the posterior segment. *J. Ocul. Pharmacol. Ther. 26*, 137−146.

(13) Lefurgy, S., and Cornish, V. (2004) Finding Cinderella after the ball: a three-hybrid approach to drug target identification. *Chem. Biol. 11*, 151−153.

(14) Kley, N. (2004) Chemical dimerizers and three-hybrid systems: scanning the proteome for targets of organic small molecules. *Chem. Biol. 11*, 599−608.

(15) Fields, S., and Song, O. (1989) A novel genetic system to detect protein-protein interactions. *Nature 340*, 245−246.

(16) Licitra, E. J., and Liu, J. O. (1996) A three-hybrid system for detecting small ligand-protein receptor interactions. *Proc. Natl. Acad. Sci. U.S.A. 93*, 12817−12821.

(17) Lin, H., Abida, W. M., Sauer, R. T., and Cornish, V. W. (2000) dexamethasone-Methotrexate: An efficient chemical inducer of protein dimerization *in vivo*. *J. Am. Chem. Soc. 122*, 4247−4248.

(18) Abida, W. M., Carter, B. T., Althoff, E. A., Lin, H., and Cornish, V. W. (2002) Receptor-dependence of the transcription read-out in a small-molecule three-hybrid system. *ChemBioChem 3*, 887−895.
(19) Becker, F., Murthi, K., Smith, C., Come, J., Costa-Roldan, N., Kaufmann, C., Hanke, U., Degenhart, C., Baumann, S., Wallner, W., Huber, A., Dedier, S., Dill, S., Kinsman, D., Hediger, M., Bockovich, N., Meier-Ewert, S., Kluge, A. F., and Kley, N. (2004) A three-hybrid approach to scanning the proteome for targets of small molecule kinase inhibitors. *Chem. Biol. 11*, 211−223.
(20) Caligiuri, M., Becker, F., Murthi, K., Kaplan, F., Dedier, S., Kaufmann, C., Machl, A., Zybarth, G., Richard, J., Bockovich, N., Kluge, A., and Kley, N. (2005) A proteome-wide CDK/CRK-specific kinase inhibitor promotes tumor cell death in the absence of cell cycle progression. *Chem. Biol. 12*, 1103−1115.
(21) Bruckner, A., Polge, C., Lentze, N., Auerbach, D., and Schlattner, U. (2009) Yeast two-hybrid, a powerful tool for systems biology. *Int. J. Mol. Sci. 10*, 2763−2788.
(22) Lentze, N., and Auerbach, D. (2008) The yeast two-hybrid system and its role in drug discovery. *Expert Opin. Ther. Targets 12*, 505−515.
(23) Althoff, E. A., and Cornish, V. W. (2002) A bacterial small-molecule three-hybrid system. *Angew. Chem., Int. Ed. 41*, 2327−2330.
(24) Henthorn, D. C., Jaxa-Chamiec, A. A., and Meldrum, E. (2002) A GAL4-based yeast three-hybrid system for the identification of small molecule-target protein interactions. *Biochem. Pharmacol. 63*, 1619−1628.
(25) Pang, I. H., Shade, D. L., Clark, A. F., Steely, H. T., and DeSantis, L. (1994) Preliminary characterization of a transformed cell strain derived from human trabecular meshwork. *Curr. Eye Res. 13*, 51−63.
(26) Liu, Y., Woods, N. T., Kim, D., Sweet, M., Monteiro, A. N., and Karchin, R. (2011) Yeast two-hybrid junk sequences contain selected linear motifs. *Nucleic Acids Res. 39*, e128.
(27) Gallant, J. A., and Lindsley, D. (1998) Ribosomes can slide over and beyond "hungry" codons, resuming protein chain elongation many nucleotides downstream. *Proc. Natl. Acad. Sci. U.S.A. 95*, 13771−13776.
(28) Chidley, C., Haruki, H., Pedersen, M. G., Muller, E., and Johnsson, K. (2011) A yeast-based screen reveals that sulfasalazine inhibits tetrahydrobiopterin biosynthesis. *Nat. Chem. Biol. 7*, 375−383.
(29) Zhang, H., Liu, X. H., Zhang, K., Chen, C. K., Frederick, J. M., Prestwich, G. D., and Baehr, W. (2004) Photoreceptor cGMP phosphodiesterase delta subunit (PDEdelta) functions as a prenyl-binding protein. *J. Biol. Chem. 279*, 407−413.
(30) Millar, J. C., Pang, I. H., Wang, W. H., Wang, Y., and Clark, A. F. (2008) Effect of immunomodulation with anti-CD40L antibody on adenoviral-mediated transgene expression in mouse anterior segment. *Mol. Vision 14*, 10−19.
(31) Shepard, A. R., Millar, J. C., Pang, I. H., Jacobson, N., Wang, W. H., and Clark, A. F. (2010) Adenoviral gene transfer of active human transforming growth factor-{beta}2 elevates intraocular pressure and reduces outflow facility in rodent eyes. *Invest. Ophthalmol. Vision Sci. 51*, 2067−2076.
(32) Shepard, A. R., Jacobson, N., Millar, J. C., Pang, I. H., Steely, H. T., Searby, C. C., Sheffield, V. C., Stone, E. M., and Clark, A. F. (2007) Glaucoma-causing myocilin mutants require the Peroxisomal targeting signal-1 receptor (PTS1R) to elevate intraocular pressure. *Hum. Mol. Genet. 16*, 609−617.
(33) Zhang, H., Hosier, S., Terew, J. M., Zhang, K., Cote, R. H., and Baehr, W. (2005) Assay and functional properties of PrBP(PDEdelta), a prenyl-binding protein interacting with multiple partners. *Methods Enzymol. 403*, 42−56.
(34) Zhang, H., Li, S., Doan, T., Rieke, F., Detwiler, P. B., Frederick, J. M., and Baehr, W. (2007) Deletion of PrBP/delta impedes transport of GRK1 and PDE6 catalytic subunits to photoreceptor outer segments. *Proc. Natl. Acad. Sci. U.S.A. 104*, 8857−8862.
(35) Rao, V. P., and Epstein, D. L. (2007) Rho GTPase/Rho kinase inhibition as a novel target for the treatment of glaucoma. *BioDrugs 21*, 167−177.
(36) Park, H. J., Kong, D., Iruela-Arispe, L., Begley, U., Tang, D., and Galper, J. B. (2002) 3-hydroxy-3-methylglutaryl coenzyme A reductase inhibitors interfere with angiogenesis by inhibiting the geranylgeranylation of RhoA. *Circ. Res. 91*, 143−150.
(37) Cook, T. A., Ghomashchi, F., Gelb, M. H., Florio, S. K., and Beavo, J. A. (2000) Binding of the delta subunit to rod phosphodiesterase catalytic subunits requires methylated, prenylated C-termini of the catalytic subunits. *Biochemistry 39*, 13516−13523.
(38) Hanzal-Bayer, M., Renault, L., Roversi, P., Wittinghofer, A., and Hillig, R. C. (2002) The complex of Arl2-GTP and PDE delta: from structure to function. *EMBO J. 21*, 2095−2106.
(39) Dadvar, P., O'Flaherty, M., Scholten, A., Rumpel, K., and Heck, A. J. (2009) A chemical proteomics based enrichment technique targeting the interactome of the PDE5 inhibitor PF-4540124. *Mol. Biosyst. 5*, 472−482.
(40) Wilson, S. J., and Smyth, E. M. (2006) Internalization and recycling of the human prostacyclin receptor is modulated through its isoprenylation-dependent interaction with the delta subunit of cGMP phosphodiesterase 6. *J. Biol. Chem. 281*, 11780−11786.
(41) Hoyng, P. F., and Groeneboer, M. C. (1989) The effects of prostacyclin and its stable analog on intraocular pressure. *Prog. Clin. Biol. Res. 312*, 369−378.
(42) Nikolova, S., Guenther, A., Savai, R., Weissmann, N., Ghofrani, H. A., Konigshoff, M., Eickelberg, O., Klepetko, W., Voswinckel, R., Seeger, W., Grimminger, F., Schermuly, R. T., and Pullamsetti, S. S. (2010) Phosphodiesterase 6 subunits are expressed and altered in idiopathic pulmonary fibrosis. *Respir. Res. 11*, 146.
(43) Bot, I., Jukema, J. W., Lankhuizen, I. M., van Berkel, T. J., and Biessen, E. A. (2011) atorvastatin inhibits plaque development and adventitial neovascularization in ApoE deficient mice independent of plasma cholesterol levels. *Atherosclerosis 214*, 295−300.
(44) Yamada, K., Sakurai, E., Itaya, M., Yamasaki, S., and Ogura, Y. (2007) Inhibition of laser-induced choroidal neovascularization by atorvastatin by downregulation of monocyte chemotactic protein-1 synthesis in mice. *Invest. Ophthalmol. Vision Sci. 48*, 1839−1843.
(45) Conrow, R. E., Dillow, G. W., Bian, L., Xue, L., Papadopoulou, O., Baker, J. K., and Scott, B. S. (2002) Corticosteroid decomposition via a mixed anhydride. *J. Org. Chem. 67*, 6835−6836.
(46) Garabedian, M. J., and Yamamoto, K. R. (1992) Genetic dissection of the signaling domain of a mammalian steroid receptor in yeast. *Mol. Biol. Cell 3*, 1245−1257.
(47) Robinson, C. R., and Sauer, R. T. (1998) Optimizing the stability of single-chain proteins by linker length and composition mutagenesis. *Proc. Natl. Acad. Sci. U.S.A. 95*, 5929−5934.